https://dx.doi.org/10.4314/jcsia.v25i2.1

nigeria computer society
ncs
www.ncs.org.ng

THE JOURNAL OF COMPUTER SCIENCE AND ITS APPLICATIONS

Vol. 25, No 2 December 2018

DEVELOPMENT OF ASPHALT PAVED ROAD POTHOLE DETECTION SYSTEM USING MODIFIED COLOUR SPACE APPROACH

A. D. Isah[1], A. M. Aibinu[2], O. M. Olaniyi[3] and O.O. Campbell[4]
[1]Niger State Polytechnic, Zungeru
[2]Federal University of Technology, Minna
[1] dagahtech@gmail.com, [2] maibinu@gmail.com, [3]Mikail.olaniyi@futminna.edu.ng, and [4]Oladelecampbell@gmail.com

ABSTRACT
Asphalt paved roads in good condition are important infrastructure that contributes to a large extent the development of a nation. The technical cost and time required to manually assess asphalt paved road conditions have limited proper and timely planning in most developing countries. This paper presents an automated pothole detection system using modified colour space technique. The modified hybrid colour space model form was used to transform the original asphalt pavement image to grey level image. The contrast of the grey level image was then enhanced to improve its visual quality and detection accuracy. The enhanced grey level image was later segmented using thresholding technique. An evaluation of the accuracy of the developed system in the detection of potholes on asphalt paved road was conducted; the result of the segmented image was compared with the ground truth under two conditions. The accuracy of 92% was obtained in the first condition where the system was able to detect potholes in the acquired image, in comprising with related literatures the detection accuracies are not given in percentages except [18] that has accuracy of 93% and is not for detecting pothole but evaluation of road defects. In [19, 20, 21, & 7] pothole detection accuracy are given as reasonable accuracy but not in percentage. Further quantitative performance analysis of the detected region was conducted using Mean Square Error (MSE) metric. The results obtained shows that the detected areas gave minimum MSE when compared with the ground truth. The research reduces the complexity of potholes detection systems using an extremely intuitive colour space model that reduces the stages involved in image processing technique for pothole detection compared with other methods from related literature which uses; 3D reconstruction method, vibration method, video images using artificial neural network models, machine vision, histogram shape based thresholding and spectral clustering from histogram data obtain from gray scale images. Some of the aforementioned methods required high cost equipment, others are computational complex because they required features extraction and training phase. The use of extremely intuitive colour space model of this paper does not required high cost equipment, filtering and training phase, hence the reduction in computational complexity of the method.

Keywords: Asphalt defects, Colour Space, Image Analysis, Performance evaluation

1.0 INTRODUCTION

Deaths and injuries resulting from defects of asphalt paved road have become a major and growing public problem around the world. Global annual death records caused by road accident have been estimated to be 1.2 million [1]. The causes of defects include ageing of the asphalt pavement, poor quality of work, and poor supervision during construction of the asphalt paved road or during maintenance of the roads, and lack of system for early detection of potholes in asphalt pavement [2, 3, 4, 5 & 6].

Pavement defects can be in form of crack; pop-outs; potholes; wear and polishing [2, 3, 4, 5 &6]. The defect of interest in this work is potholes. Potholes are the most common form of road defects that can easily be seen in most asphalt paved roads in Nigeria [7]. Lost incurred due to asphalt pavement defects in Nigeria is estimated to be 80 billion naira per annum [8 & 9], thus, necessitating government putting in place agency saddled with the responsibility of monitoring and maintaining road conditions [10]. Even with this agency in place, the rate of defects on the asphalt paved roads in Nigeria is still 65% [11], because the cost and time required to manually asses asphalt pavement condition limit proper planning of repairs and rehabilitation of the roads. Hence, an automated potholes detection technique using digital image processing technique is been sought in this work.

Digital image processing technique is used in this research for pothole detection in an asphalt paved road using mathematical operations to transform image for analyses and detection. The Digital image processing stages include colour space conversion, contrast enhancement, segmentation and binarization. Generally, digital image processing techniques from related literature follow this format [12]. This research work formulates colour space model for segmenting asphalt pavement images for pothole image detection. The work is organized into five sections. Section one is the introduction, section two literature review, section three methodology, section four result analysis and section five conclusion.

1. LITERATURE REVIEW

Various techniques have been reported in the literature for detecting potholes on asphalt paved road. Figure 1 is the classification of various pothole detection techniques. The manual and semi-automated techniques are time-consuming and costly task, while the automated detection technique has been used in asphalt pavement defects detection and found to be effective and efficient. 3D reconstruction of the automated technique requires high-cost laser scanners, while vibration is not reliable when the surface vibrates, such as bridge expansion joints. The vision-based approach relies on image processing analysis [6, 7 & 14].

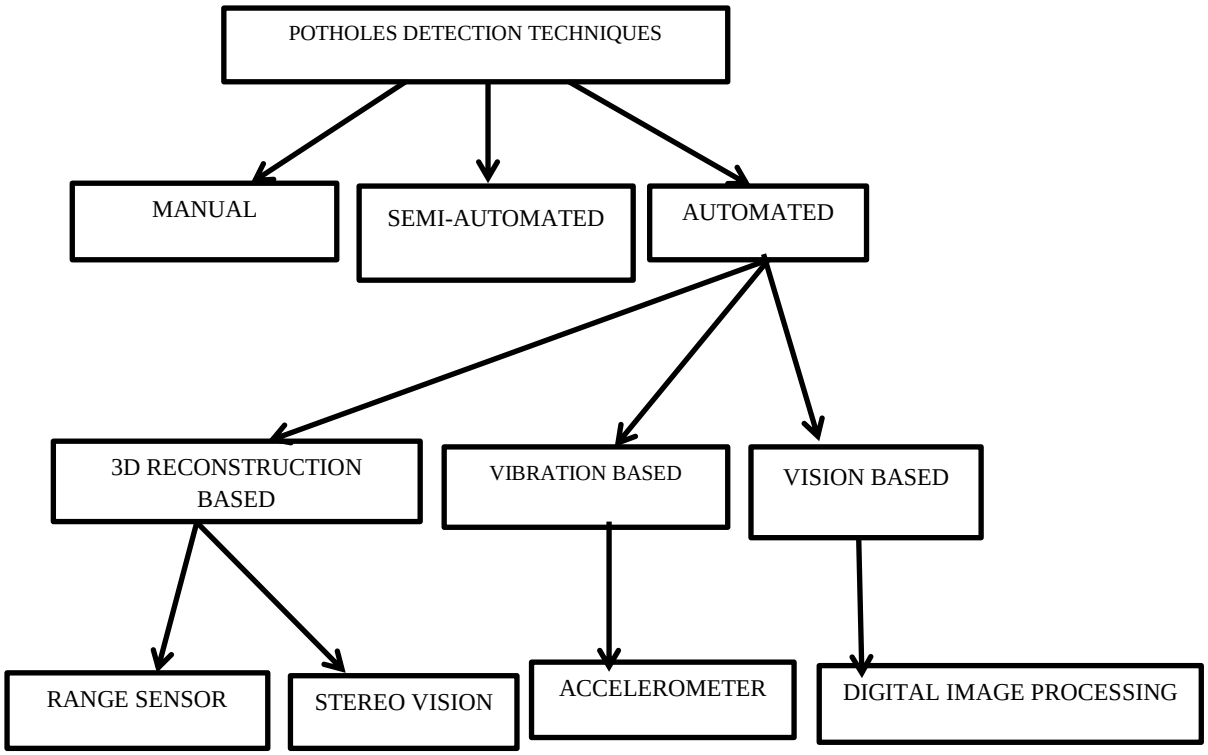

Figure 1: Classification of potholes detection techniques

This paper uses digital image processing technique for pothole detections. A number of related works exist in the application of digital image processing to object defects in the different problem domain. In [18], an automated methodology of processing highway pavement defects using video images by using artificial neural network models with image-processing methods was presented. The technique successfully classifies the crack of the pavement based on severity, and extent of cracks detected in the video images. The technique is based on five major steps which include: image segmentation, feature extraction, decomposition of the image, classification of cracking, and computation of the severities and extents of cracking detected in each image. The technique was able to detect, classify, and quantify highway pavement surface cracks.

Similarly, [19] present an algorithm for evaluating alligator, transverse, longitudinal, block cracking and pothole. The algorithm first binarizes the pavement image and then divides the image into sub-images. The classification rules were based on neural network technique which classifies the sub-images as linear, jointed, pothole, and non-damaged. Seventy images database was formed and used for evaluating the developed algorithm. The experimental result shows that the algorithm recognizes 100 percent for cracking and 93 percent for potholes.

Furthermore, [20] proposed a method that uses machine vision to detect potholes in asphalt pavement images of highway using structured illumination to generate low-resolution edge map that initializes active contour maps that synthesize the final image. Two lower resolution intensity images formed from the original image by subdividing the image. Two candidate edge points were generated in the lower resolution image layer by masking the image with a filter that matched the expected width of the light stripe edge points were selected based on the response that is equivalent to the number of projection as the candidate edge points. Maximum edge contour was formed using each stripe of the second image layer and transformed to the first image layer. The

position of each edge point was reformed by searching for a limited spatial domain in the first layer which was constrained by internal and external energy functions. The set of maximum snakes was transfer to higher resolution layer the process was repeated. The technique estimate pothole sizes with high accuracy.

In another related work, [21] developed an automated algorithm for pothole detection. The texture was measured based on the histogram extracted as the features of the image region, and a non-linear support vector machine was built to identify whether a target region is a pothole or a non-pothole region. The experimental result shows that the algorithm achieved a high recognition rate. Similarly, [5 & 14] presented a method for automated pothole detection in asphalt pavement images. The technique segmented images into the defect and non-defect regions using histogram shape-based thresholding technique. Based on the geometric properties of a defect region the potential pothole shape was approximated utilizing morphological thinning and elliptic regression. Subsequently, the texture inside a potential defect shape was extracted and compared with the texture of the surrounding non-defect pavement in order to determine if the region of interest represents pothole. The methodology was implemented using MATLAB software with 120 pavement images. The experimental results show that the technique can detect potholes in asphalt paved road with reasonable accuracy.

In [7], an unsupervised technique for identification of potholes by estimating it surface using image analysis and spectral clustering from histogram data obtained from the grey-scaled image was presented. The technique does not require additional filtering and training phase. The experimental results show that the techniques detected potholes with reasonable accuracy.

The review of the related literature of pothole detection techniques using image processing techniques carried out in this works reviled their computational complexity this is attributed to stages involved which include; image acquisition, image conversion, image contrast enhancement, segmentation, feature extraction and object recognition. The aforementioned literature did not look at the characteristics of the various colour spaces, this leads to the use of image filtering and enhancement to get a better image for further processing this increase the stages of image processing techniques. Hence, the increase in computational complexity of the pothole detection system using images processing technique that has been carried out in the related literature review in this research.

This paper aims at reducing the computational complexity of pothole detection system using image processing technique by looking at the characteristics of the various colour spaces and choosing the one that has good characteristics that can be used for reducing the stages involved in image processing technique for pothole detection.

Colour space is a scheme of specifying colour in the Human Visual System (HVS) due to the fact that human visual system cannot see all the visible electromagnetic spectrum approximated in the range of 300 to 830nm because of certain characteristics of HVS [13]. The effectiveness of colour spaces in different applications is not the same, for example, some equipment has restraining factors that dictate the size and type of colour space that can be used. Some colour spaces are perceptually linear which means ten unit change in stimulus will produce the same change in perception wherever it is applied. Many colour spaces, particularly in computer graphics, are not linear in this way. Some colour spaces are intuitive to use, which means it is easy for the user to navigate within them and creating desired colours is relatively easy.

Other spaces are confusing for the user with parameters with abstract relationships to the perceived colour. Finally, some colour spaces are tied to a specific piece of equipment, which means they are device dependent while others are equally valid on whatever device they are used, choice of colour space has an effect on the result of digital image processing [13 & 14]. There is numerous colour space but the commonly used are RGB; CMY; YUV; YIQ; YPbPr; YCbCr; YCgCr; YDbDr; HSV or HSI, and CIE-XYZ [15]. Table 1 provides the comparison of the commonly used colour space in digital image processing and their characteristics. Red, Green, and Blue (RGB) is an additive model which all colours are created from [12, 13, 14 & 15]. RGB colour space is not robust when lighting conditions changes and it is non-intuitive meaning that it is not easy to navigate them and create desired colour [12]. This lack of intuitivism characteristic is what is lacking in most of the colour space in Table 1 except Hue, Saturation, and Value (HSV) colour space which is extremely intuitive. Extreme intuitive property of HSV colour space makes it suitable for use in digital image processing, hence its choice for use in this research.

Hue, Saturation, and Lightness (HSL) were the L (lightness) replaces V (Value) are model proposed in [12]. Hue, Saturation, and Intensity (HSI) colour uses intensity rather than value to represent lightness is a model proposed by Gonzalez and Woods [12 & 13]. HSV and HSI colour space is more efficient in handling an image with shadows thus make it robust to change due to illumination [16]. The mathematical definition for transforming RGB colour scheme to other colour space models are given in equations 1 to 10 [12, 15 & 17], which were used to formulate algorithm and apply to asphalt pavement image to justify Table 1 and result presented in section four

.

Table 1: Comparison of commonly used colour space

	CHARACTERISTICS				
Colour space model	Area of application	Model	Transformation	Device dependent	Intuitism
RGB	Display Technology using CRT	Additive	Linear	Yes	Non-intuitive
CMY	Printing Application	Subtractive	Non-linear	Yes	Quite unintuitive
YUV	Used for analogue television such as PAL or NTSC	Subtractive	Linear	Yes	Quite unintuitive
YIQ	Used for analogue television such as PAL or NTSC	Subtractive	Linear	Yes	Quite unintuitive
YPbPr	Used for analogue television such as PAL or NTSC	Subtractive	Linear	Yes	Quite unintuitive
YCbCr	Used for digital video encoding	Subtractive	Linear	Yes	Quite unintuitive
YCgCr	Used for digital video encoding	Subtractive	Linear	Yes	Quit unintuitive
YDbDr	Used for analogue television such as PAL or NTSC	Subtractive	Linear	Yes	Quite unintuitive
HSV or HSI	Used by artist	Depth purity and brightness	Linear	No	Extremely intuitive
CIE-XYZ	Display technology using CRT	Human vision	Nearly linear	No	Quite unintuitive

$CMY = \{1 - R, 1 - G, 1 - B\}$ (1) [12, 15 & 17].

$$YUV = \begin{Bmatrix} +0.299R + 0.587G + 0.114B \\ -0.14713R - 0.28886G + 0.436B \\ +0.615R - 0.51499G - 0.10001B \end{Bmatrix} \quad (2)$$ [12, 15 & 17].

$$YIQ = \begin{Bmatrix} 0.299R + 0.587G + 0.114B \\ 0.595716R - 0.274453G - 0.321263B \\ 0.211456R - 0.522591G + 0.311134B \end{Bmatrix} \quad (3)$$ [12, 15 & 17].

$$YPbPr = \begin{Bmatrix} 0.299R + 0.587G + 0.114B \\ -0.168736R - 0.331264G + 0.5B \\ 0.5R - 0.418688G - 0.081312B \end{Bmatrix} \quad (4)$$ [12, 15 & 17].

$$YCbCr = \begin{Bmatrix} 16 + \frac{1}{256} * (65.738R + 129.057G + 25.064B \\ 128 + \frac{1}{256} * (-37.945R - 74.494G + 112.439B \\ 128 + \frac{1}{256} * (112.439R - 94.154G - 18.285B \end{Bmatrix} \quad (5)$$ [12, 15 & 17]

$$YCgCr = \begin{Bmatrix} 16 + 65.481R + 128.553G + 24.966B \\ 128 - 81.085R + 112G - 30.915B \\ 128 + 112R - 93.768G - 18.214B \end{Bmatrix} \quad (6)$$ [12, 15 & 17].

$$YDbDr = \begin{Bmatrix} 0.299R + 0.587G + 0.114B \\ -0.450R - 0.883G + 1.333B \\ -1.333R + 1.116G + 0.217B \end{Bmatrix} \quad (7)$$ [12, 15 & 17].

$$CIE = \begin{Bmatrix} 0.490186R + 0.309879G + 0.199934B \\ 0.177015R + 0.812324G + 0.010660B \\ 0.010077G + 0.989922B \end{Bmatrix} \quad (8)$$ [12, 15 & 17

$$HSV = \begin{Bmatrix} Undefine, if \max(R,G,B) = \min(R,G,B \\ 60X \frac{G-B}{\max(R,G,B) - \min(R,G,B)} + 0, if \max(R,G,B) = R \; and \; G \geq B \\ 60X \frac{G-B}{\max(R,G,B) - \min(R,G,B)} + 360, if \max(R,G,B) = R \; and \; G < B \\ 60X \frac{B-R}{\max(R,G,B) - \min(R,G,B)} + 120, if \max(R,G,B) = G \\ 60X \frac{R-G}{\max(R,G,B) - \min(R,G,B)} + 240, if \max(R,G,B) = B \\ 1 - \left(\frac{min(R,G,B)}{\max(R,G,B}\right) \\ max(R,G,B) \end{Bmatrix} \quad (9)$$ [12, 15 & 17].

$$HSI = \begin{Bmatrix} cos^{-1}\left(\frac{0.5(R-G)+(R-B)}{\sqrt{(R-G)^2+(R-B)(G-B)}}\right) \\ 1 - \left(\frac{3}{R+G+B}\right)\min(R,G,B) \\ \frac{R+G+B}{3} \end{Bmatrix} \quad (10)$$ [12, 15 & 17],

2. METHODOLOGY

Colour space model was formulated in this work by a hybrid of saturation components of Hue-Saturation-Value (HSV) colour space model defined in equation 9 with saturation components of Hue-Saturation-Intensity (HSI) colour space model defined in equation 10. The formulated colour space model is defined in equation 13, which is used to transform the original asphalt pavement images in RGB scheme to grey scheme.

$$S_{HSV} = 1 - \left(\frac{\min(R,G,B)}{\max(R,G,B)}\right) \quad (11)$$

$$S_{HSI} = 1 - \left(\left(\frac{3}{R+G+B}\right)\min(R,G,B)\right) \quad (12)$$

Equation 11 hybrid with equation 12 and the constant value three replaced with variable 'K' to give the formulated equation 13

$$S_{HYBRID} = 1 - \left(\left(\frac{K}{R+G+B}\min(R,G,B)\right) * \left(\frac{\min(R,G,B}{\max(R,G,B}\right)\right) \quad (13)$$

In determining the optimal value for K in equation 13, the value was varied from 3 to 3.5 to obtained optimal co-efficient.

The transformed asphalt pavement images contrast were enhanced to improved visual quality of the images using histogram equalization defined in equation 14.

$$g(x,y) = \frac{m-1}{\sum_{j=i}^{m} n_j} \sum_{j=i}^{f(x,y)} n_j \quad (14)$$

Where m is the total number of grey levels in the image to be enhanced$f$, n_j is the number of pixels having particular gray level j and i ranges from 0 to 255.

Histogram based thresholding was used in this work for segmentation based on the assumption that asphalt pavement image has two gray levels, the gray level associated with the normal asphalt pavement and the gray level associated with the pothole. Based on this assumption the histogram based thresholding partition the pixels based on the intensity value of the normal pavement and pothole images to give two peaks. The process of the histogram based thresholding was achieved by setting intensity values thresholds (T) define in equation 15. Based on the value of T, the asphalt pavement image with pothole is converted from a segmented image s (x, y) to a binary image. Thresholding mapped grayscale into binary set {0, [22].

$$s(x,\ y) = \{^{1, if\ g(x,Y) < T(x,y)}_{0, if\ g(x,y) \geq T(x,y)} \quad (15)$$

Where $s(x, y)$the value of the segmented image $g(x, y)$ is the enhanced gray level of the pixel (x, y) and $T(x, y)$ is the threshold value at the coordinate(x, y). Single threshold value of 0.2 from a normalized intensity image as the appropriate threshold value

Performance evaluation measures how efficient the pothole detection algorithm developed in this research work performed on a number of images in a database. In this research, the performance of the pothole detection system algorithm was tested using Mean Square Error (MSE) define in Equation 16. A database of thirty-five different asphalt pavements with potholes images and twenty-five normal asphalt pavement image acquired was formed and used for the performance evaluation in this researched. Truth images of the sixty images in the database were also form using Adobe Photoshop for making a comparison with the segmented pothole image using the algorithm developed, the result of the implementation is presented in section 4.

$$MSE = \frac{1}{MXN}\sum_{i=1}^{M}\sum_{j=1}^{N}[b(i,j) - \acute{b}(i,j)]^2 \quad (16)$$

Where M, N are the number of rows and columns of the compared images matrix, $b(i, j)$ is the pixel value of the segmented image using the developed algorithm and $b(\acute{i}, j)$ is the pixel value of the truth image. The developed pothole detection system of this researched employs block diagram of figure 2

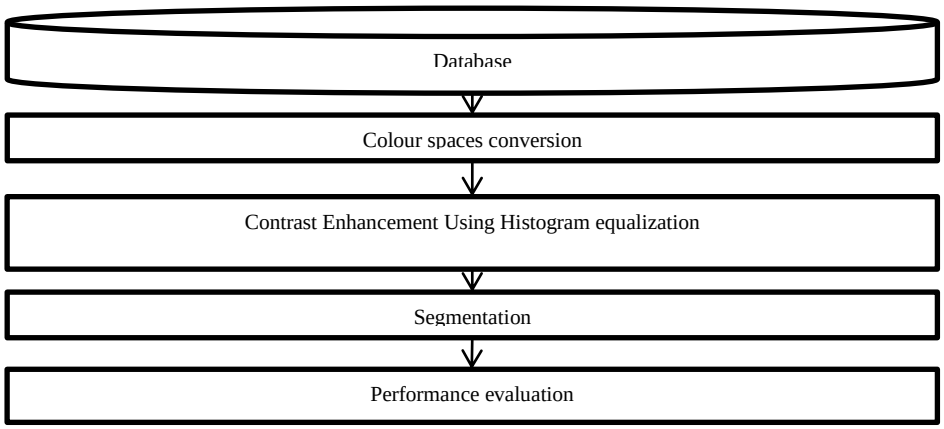

Figure 2: Block diagram of an asphalt paved road potholes detection system

3.1 System implementation

The algorithm for pothole detection in asphalt paved road was implemented as follow:

1. Start
2. $Input\ R, G, B, K, S_{HYBRID}$
3. $Computer\ S_{HYBRID} = 1 - \left(\left(\frac{K}{R+G+B}\min(R,G,B)\right) * \left(\frac{\min(R,G,B}{\max(R,G,B)}\right)\right)$
4. $Input\ x, y, m, n, i, j, M, N$
5. $Compute\ g(x,y) = \frac{m-1}{\sum_{j=i}^{m} n_j}\sum_{j=i}^{f(x,y)} n_j$
6. $Compute\ s(x,\ y) = \begin{cases} 1, if\ g(x,Y) < T(x,y) \\ 0, if\ g(x,y) \geq T(x,y) \end{cases}$
7. $Compute\ MSE = \frac{1}{MXN}\sum_{i=1}^{M}\sum_{j=1}^{N}[b(i,j) - \acute{b}(i,j)]^2$
8. $Stop$

3. RESULT ANALYSIS

a. Database of images

Sixty images were acquired and used to create a database and to form the ground truth images using Adobe Photoshop. Figure 3 shows a sample of five images in the database and the ground truth

Figure 3: Sample of five images used in the study (row1) and the ground truth image generated for each one (row2)

b. The
c. result of the transform RGB colour space using most common colour spaces models

The result of the most used colour space CMY, YUV, YIQ, YPbPr, YCbCr, YCgCr, YDbDr, CIE, HSV, and HSI discussed in section 2 are presented in this section using mathematical definitions of equations 1 – 10 to transform and select the best to be used based on visual appearance. Figure 4 is the result of transform RGB images using CMY, discussed in section 2; the pothole and the normal pavement in the images of all the channels do not show clear distinction for segmentation. Figures 5-7, and 10, are results of transform RGB image using YUV, YIQ, YPbPr, and YDbDr; their outputs are the same with CMY. The pothole and the normal pavement in the images of all the channels do not show clear distinction for segmentation. Figure 8 is the transformed image using YCbCr, the pothole and the normal pavement in the images of all the channels do not show clear distinction for segmentation. Figure 9 is the transformed image using YCgCr all the channels are white which cannot be used for

segmentation. Figure 11 is the transformed image using CIE; the pothole and the normal pavement of the asphalt pavement image do not show clear distinction for segmentation. Figure 12 is transformed RGB image using HSV/HIS and hybrid colour space models; there is a distinction in the pothole and the normal pavement background which enables segmentation of the image by choosing common pixel value. Figure 13 is the segmented output images using the formulated hybrid colour space mode, while Figure 14 is the segmented output images using coefficient value of 3.3 if compared to the true image of Figure 15. The segmented image using coefficient value of 3.3 from the hybrid image is similar.

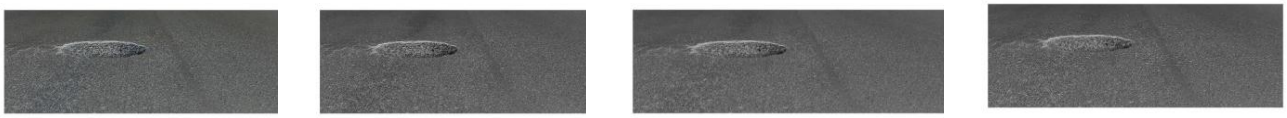

Figure 4: Original RGB image transform using CMY colour space model

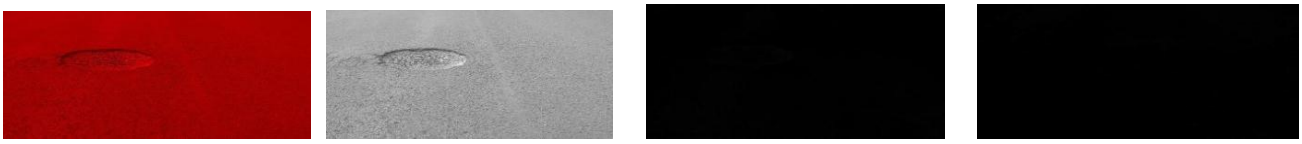

Figure 5: Original RGB image transform using YUV colour space model

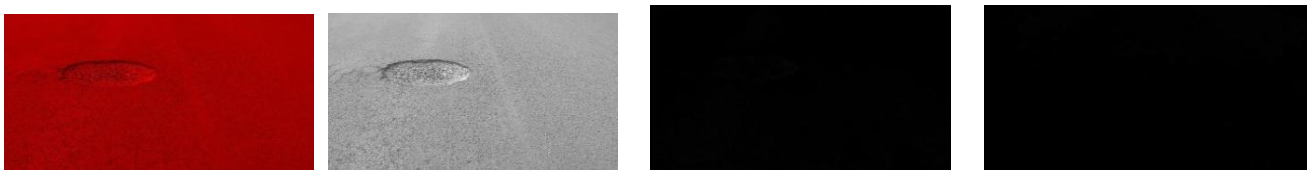

Figure 6: Original RGB image transform using YIQ colour space model

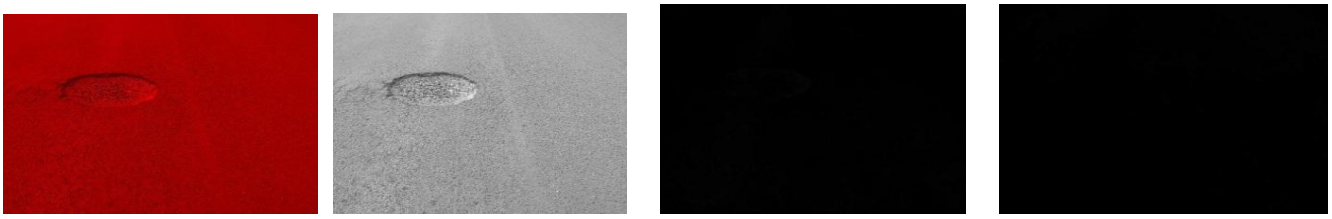

Figure 7: Original RGB image transform using YPbPr colour space model

Figure 8: Original RGB image transform using YCbCr colour space model

White output in all the channels

Figure 9: Original RGB image transform using YCgCr colour space model

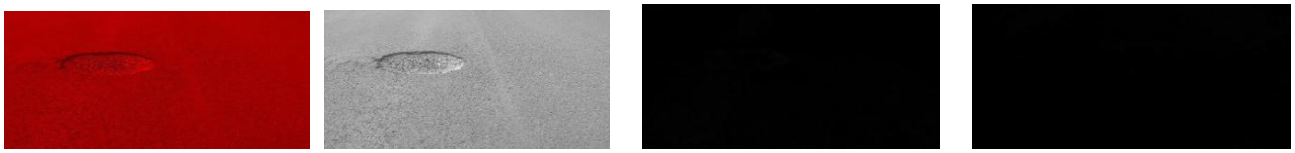

Figure 10: Original RGB image transform using YDbDr colour space image

Figure 11: Original RGB image transform using CIE colour space model

Figure 12: Original RGB image transform using HSV, HSI, and Hybrid colour space model

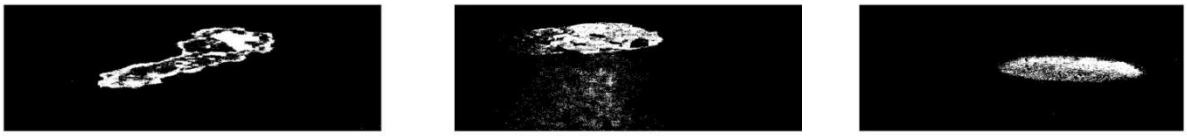

Figure 13: Output of segmented images using the formulated hybrid colour space model

Figure 14: Output of segmented images using the coefficient value of 3.3

Figure 15: Truth images formed using Adobe Photoshop

4.1 Performance evaluation of the developed system

Detection accuracy of the developed system was done by testing the developed algorithm on sixty captured asphalt paved road images, thirty-five with potholes and twenty-five without potholes. Thirty-tree images with potholes were accurately detected and twenty-two without potholes were accurately detected without potholes with the results shown in Table 2.

Table 2: Detection Accuracy

S/N	Type of Pavement Image	Result of detection
1	Pothole	Algorithm detected the Pothole
2	Pothole	Algorithm detected the Pothole
3	Pothole	Algorithm detected the Pothole
4	Pothole	Algorithm detected the Pothole
5	Pothole	Algorithm detected the Pothole
6	Pothole	Algorithm detected the Pothole
7	Pothole	Algorithm detected the Pothole
8	Pothole	Algorithm detected the Pothole
9	Pothole	Algorithm detected the Pothole
10	Pothole	Algorithm detected the Pothole
11	Pothole	The algorithm did not detect the Pothole
12	Pothole	Algorithm detected the Pothole
13	Pothole	Algorithm detected the Pothole
14	Pothole	Algorithm detected the Pothole
15	Pothole	Algorithm detected the Pothole
16	Pothole	Algorithm detected the Pothole
17	Pothole	The algorithm did not detect the Pothole
18	Pothole	Algorithm detected the Pothole
19	Pothole	Algorithm detected the Pothole
20	Pothole	Algorithm detected the Pothole
21	Pothole	Algorithm detected the Pothole
22	Pothole	Algorithm detected the Pothole
23	Pothole	Algorithm detected the Pothole
24	Pothole	Algorithm detected the Pothole
25	Pothole	Algorithm detected the Pothole
26	Pothole	Algorithm detected the Pothole
27	Pothole	Algorithm detected the Pothole
28	Pothole	Algorithm detected the Pothole
29	Pothole	Algorithm detected the Pothole
30	Pothole	Algorithm detected the Pothole
31	Pothole	Algorithm detected the Pothole
32	Pothole	Algorithm detected the Pothole
33	Pothole	Algorithm detected the Pothole
34	Pothole	Algorithm detected the Pothole
35	Pothole	Algorithm detected the Pothole
1	Non-Pothole	There is Pothole
2	Non-Pothole	There is no Pothole
3	Non-Pothole	There is no Pothole
4	Non-Pothole	There is no Pothole
5	Non-Pothole	There is no Pothole
6	Non-Pothole	There is no Pothole
7	Non-Pothole	There is no Pothole
8	Non-Pothole	There is no Pothole
9	Non-Pothole	There is no Pothole
10	Non-Pothole	There is no Pothole
11	Non-Pothole	There is no Pothole
12	Non-Pothole	There is no Pothole
13	Non-Pothole	There is no Pothole
14	Non-Pothole	There is Pothole
15	Non-Pothole	There is no Pothole
16	Non-Pothole	There is no Pothole
17	Non-Pothole	There is no Pothole
18	Non-Pothole	There is no Pothole
19	Non-Pothole	There is no Pothole
20	Non-Pothole	There is no Pothole
21	Non-Pothole	There is no Pothole
22	Non-Pothole	There is no Pothole
23	Non-Pothole	There is no Pothole
24	Non-Pothole	There is Pothole
25	Non-Pothole	There is no Pothole

The accuracy of detection computed using: $Accuracy = \frac{TP+TN}{P+N} X100\%$ [26] [17] where $TP =$ Total image with pothole detected, $TN =$ Total image without Pothole detected, $P =$ Total number of images with pothole, and $N =$ Total number of images without pothole.

$Accuracy = \frac{33+22}{35+255} X100 = \frac{55}{60} X100 = 92\%$

a. Performance Analysis of Detected Areas

The performance evaluation of the algorithm developed for the detection of a pothole in asphalt paved road was evaluated using MSE metrics. The best threshold value obtained was 0.2 and coefficient value 'K' was 3.3 based on the computed means square error value. Tables 3 -7 are the computed values of MSE using the various threshold values and coefficient values. From the Tables, the means square errors values of Table 4 have the smallest values compared to Tables 3, 5, 6 and 7.

Table 3: Computed values of MSE with a threshold value of 0.1

IMAGES	CO-EFFICIENT VALUES					
	3	3.1	3.2	3.3	3.4	3.5
1	0.1290	0.1290	0.0741	0.0741	0.0741	0.0741
2	0.1416	0.1416	0.0626	0.0626	0.0626	0.0626
3	0.1393	0.1393	0.0574	0.0574	0.0574	0.0574
4	0.1223	0.1223	0.0598	0.0598	0.0598	0.0598
5	0.0800	0.0800	0.0163	0.0163	0.0163	0.0163
6	0.0946	0.0946	0.0441	0.0441	0.0441	0.0441
7	0.0741	0.0741	0.0390	0.0390	0.0390	0.0390
8	0.1089	0.1089	0.0654	0.0654	0.0654	0.0654
9	0.1379	0.1379	0.0233	0.0233	0.0233	0.0233
10	0.0269	0.0269	0.0179	0.0179	0.0179	0.0179

Table 4: Computed values of MSE with a threshold value of 0.2

IMAGES	CO-EFFICIENT VALUES					
	3	3.1	3.2	3.3	3.4	3.5
1	0.1104	0.0730	0.0686	0.0686	0.0687	0.0688
2	0.0803	0.0580	0.0328	0.0209	0.0179	0.0175
3	0.0748	0.0481	0.0253	0.0178	0.0161	0.0159
4	0.0807	0.0541	0.0284	0.0171	0.0141	0.0138
5	0.0416	0.0163	0.0138	0.0173	0.0211	0.0242
6	0.0635	0.0431	0.0294	0.0246	0.0238	0.0245
7	0.0362	0.0330	0.0338	0.0374	0.0414	0.0450
8	0.0710	0.0577	0.0507	0.0483	0.0494	0.0509
9	0.0392	0.0185	0.0100	0.0076	0.0083	0.0092
10	0.0204	0.0179	0.0181	0.0186	0.0188	0.0188

Table 5: Computed values of MSE with a threshold value of 0.3

IMAGES	CO-EFFICIENT VALUES					
	3	3.1	3.2	3.3	3.4	3.5
1	0.0687	0.0687	0.0687	0.0687	0.0688	0.0686
2	0.0182	0.0182	0.0182	0.0182	0.0176	0.0220
3	0.0162	0.0162	0.0162	0.0162	0.0160	0.0183
4	0.0147	0.0147	0.0147	0.0147	0.0143	0.0184
5	0.0216	0.0216	0.0216	0.0216	0.0249	0.0173
6	0.0247	0.0247	0.0247	0.0247	0.0254	0.0257
7	0.0417	0.0417	0.0417	0.0417	0.0452	0.0372
8	0.0496	0.0496	0.0496	0.0496	0.0513	0.0483
9	0.0085	0.0085	0.0085	0.0085	0.0094	0.0075
10	0.0188	0.0188	0.0188	0.0188	0.0188	0.0187

Table 6: Computed values of MSE with a threshold value of 0.4

IMAGES	CO-EFFICIENT VALUES					
	3	3.1	3.2	3.3	3.4	3.5
1	0.0688	0.0688	0.0688	0.0688	0.0688	0.0688
2	0.0176	0.0176	0.0176	0.0176	0.0176	0.0176
3	0.0160	0.0160	0.0160	0.0160	0.0160	0.0160
4	0.0150	0.0150	0.0150	0.0150	0.0150	0.0150
5	0.0261	0.0261	0.0261	0.0261	0.0261	0.0261
6	0.0266	0.0266	0.0266	0.0266	0.0266	0.0266
7	0.0459	0.0459	0.0459	0.0459	0.0459	0.0459
8	0.0517	0.0517	0.0517	0.0517	0.0517	0.0517
9	0.0097	0.0097	0.0097	0.0097	0.0097	0.0097
10	0.0189	0.0189	0.0189	0.0189	0.0189	0.0189

Table 7: Computed values of MSE with a threshold value of 0.5

IMAGES	CO-EFFICIENT VALUES					
	3	3.1	3.2	3.3	3.4	3.5
1	0.0689	0.0689	0.0689	0.0689	0.0689	0.0689
2	0.0177	0.0177	0.0177	0.0177	0.0177	0.0177
3	0.0160	0.0160	0.0160	0.0160	0.0160	0.0160
4	0.0163	0.0163	0.0163	0.0163	0.0163	0.0163
5	0.0303	0.0303	0.0303	0.0303	0.0303	0.0303
6	0.0292	0.0292	0.0292	0.0292	0.0292	0.0292
7	0.0487	0.0487	0.0487	0.0487	0.0487	0.0487
8	0.0538	0.0538	0.0538	0.0538	0.0538	0.0538
9	0.0105	0.0105	0.0105	0.0105	0.0105	0.0105
10	0.0189	0.0189	0.0189	0.0189	0.0189	0.0189

4. CONCLUSION

We have studied various road defects in asphalt paved roads and found pothole to be the most common road defects seen on most roads in Nigeria. Also, various methods of pothole detections techniques have also been reviewed. From the review, the automated technique using image processing was found to be cost-effective and has excellent accuracy in detecting potholes in asphalt pavement images. Therefore, the research used image processing technique for pothole detection in asphalt paved road. The methodology used in this work involves formulating hybrid colour space model using the saturation channel of HSV/HSI colour space model based on their extreme intuitive characteristics. The formulated colour space model was then used to transform RGB image to grey level image. The grey image was later segmented using simple thresholding technique. The selection of the threshold value was based on the performance evaluation criteria of MSE. The developed algorithm was implemented on a database of sixty different asphalt pavements images. The performance of the developed system was evaluated using MSE metric. The values obtained using the MSE metric was small indicating computational accuracy of the developed system. The developed system will solve the problem of cost and time required to manually assess asphalt pavement condition that has limited proper planning of repairs and rehabilitation in some of the developed countries such as Nigeria. This research has contributed to knowledge by formulating colour space model that can be used in digital image processing related problems.

6.

REFERENCES

[1] M. Peden, R. Scurfield, D. Sleet, D. H. A. Mohan, E. Jarawan. World report on road traffic prevention: World Health Organization Geneva, 2004.

[2] T. P. Barrette. *Comparison of PASER and PCI Pavement Distress Indices.* Master's Report. Michigan Technological University. Michigan, 2011.

[3] S. Cafiso, A. Graziano, S. Battiato. *Evaluation of pavement surface distress using digital image collection and analysis.* ." In International Congress on Advances in Civil Engineering, 7(11) (2006) 1-10.

[4] C. Koch, G. M. Jog, I. Brilakis. Automated pothole distress assessment using asphalt pavement video data. *Journal of Computing in Civil Engineering*. 27(4) (2013) 370–378.

[5] C. Koch, I. Brilakis. Pothole detection in asphalt pavement images. *Advanced Engineering Informatics, 25*(3) (2011) 507-515.

[6] S. Radopoulou, G. Jog, I. Brilakis. *Patch Distress Detection in Asphalt Pavement Images.* Paper presented at the 30th International Symposium on Automation and Robotics in Construction (ISARC 2013). Montreal, Canada.

[7] E. Buza, S. Omanovic, A. Huseinovic. *Pothole Detection with Image Processing and Spectral Clustering.* Paper presented at the 2nd International Conference on Information Technology and Computer Networks (ITCN 2013), Antalya, Turkey.

[8] A. O. Atubi. Identification of cycles and periodic Oscillations of Road Traffic Accidents over Lagos State, Nigeria. [Special Issue]. *International Journal of Humanities and Social Science, 2*(24) (2012) 312 - 327.

[9] M. Labinjo, C. Juilliard, O. Kobusingye, A.A. Hyder. The burden of road traffic injuries in Nigeria: results of a population-based survey. *Injury*

Prevention, 15(3), (2009) 157-162.

[10] 0.0. Lanre. Optimizing Post-Construction Lifeline of the Nigerian Road Network System: Failures and Causes, Preventions and Remedies. *J. Eng. Applied Sci, 1*(4), (2006) 456-461.

[11] O. Oke, J. Aribisala, O. Ogundipe, O. Akinkurolere. Recycling of asphalt pavement for accelerated and sustainable road development in Nigeria. *Int J Sci Technol Res, 2*(7) (2013) 92-98.

[12] C. Rafael, R. E. W. Gonzalez. Digital Image Processing. Pearson Education Press UK, 2002.

[13] M. Tkalcic J. F. Tasic. *Colour spaces: perceptual, historical and applicational background.* Paper presented at the Eurocon, 2003. Available at: http://dx.doi.org/10.1109/EURCON.2003. 1248032. Retrieved on 20/04/2015

[14] A. Ford, A, Roberts. Colour space conversions. *Westminster University, London,1998* 1-31.

[15] J. M. Chaves-González, M. A. Vega-Rodríguez, J. A. Gómez-Pulido, J. M. Sánchez-Pérez. Detecting skin in face recognition systems: A colour spaces study. *Digital Signal Processing, 20*(3) (2010) 806-823.

[16] J. Huang, B. Kong, B. Li, F. Zheng. *A new method of unstructured road detection based on HSV colour space and road features.* Paper presented at the Information Acquisition, 2007. ICIA'07. International Conference on Information Acquisition. Seogwipo-is, 2007, 596-601

[17] A. Hanbury. Constructing cylindrical coordinate colour spaces. *Pattern Recognition Letters, 29*(4) (2008) 494-500.

[18] M. S. Kaseko, S. G. Ritchie. A neural network-based methodology for pavement crack detection and classification. *Transportation Research Part C: Emerging Technologies, 1*(4) (1993) 275- 291.

[19] C. -P. J. Chou, T –K. Liau. Development of automated algorithms for pavement condition survey. *Transportation Research Record: Journal of the Transportation Research Board, 1536*(1) (1996) 103-109.

[20] A. Grace, D. Pycock, H. T. Tillotson, M. S. Snaith. Active shape from stereo for highway inspection. *Machine Vision and Applications, 12*(1) (2000) 7-15.

[21] J. Lin, Y. Liu. *Potholes detection based on SVM in the pavement distress image.* Paper presented at the Ninth International Symposium on Distributed Computing and Applications to Business, Engineering and Science. Hong Kong, 2010.

[22] M. P. Ekstrom, M. P. *Digital image processing techniques* . Academic Press. Vol 2. 2012.

[23] A. Chadha, N. Satam. An Efficient Method for Image and Audio Steganography using Least Significant Bit (LSB) Substitution, 2013. *arXiv preprint arXiv:1311.1083.*

[24] H. Gupta, R. Kumar, S. Changlani. Enhanced Data Hiding Capacity Using LSB-Based Image Steganography Method. *International Journal of Emerging Technology and Advanced Engineering,* 2013, 2250-2459.

[25] S. A. Laskar, K. Hemachandran. High Capacity data hiding using LSB Steganography and Encryption. *International Journal of Database Management Systems (IJDMS),4(6) (2012)* 57-68

[26] A. M. Aibinu, M.J.E. Salami, A.A. Shafie, A. A. Retina fundus image mask generation using pseudo parametric modelling technique. IIUM Engineering Journal, 11(2) (2010) 163 – 177.